



**CHALMERS**  
UNIVERSITY OF TECHNOLOGY

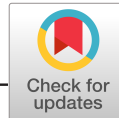
## **Evolution of surface chemistry during sintering of water-atomized iron and low-alloyed steel powder**

Downloaded from: <https://research.chalmers.se>, 2023-05-04 23:32 UTC

Citation for the original published paper (version of record):

Wendel, J., Manchili, S., Cao, Y. et al (2020). Evolution of surface chemistry during sintering of water-atomized iron and low-alloyed steel powder. *Surface and Interface Analysis*, 52(12): 1061-1065. <http://dx.doi.org/10.1002/sia.6852>

N.B. When citing this work, cite the original published paper.



# Evolution of surface chemistry during sintering of water-atomized iron and low-alloyed steel powder

Johan Wendel | Swathi K. Manchili | Yu Cao | Eduard Hryha |  
Lars Nyborg

Department of Industrial and Materials  
Science, Chalmers University of Technology,  
Gothenburg, Sweden

## Correspondence

Johan Wendel, Department of Industrial and  
Materials Science, Chalmers University of  
Technology, Gothenburg, Sweden.  
Email: johan.wendel@chalmers.se

## Funding information

Swedish Foundation for Strategic Research

Water-atomized iron and steel powder is commonly used as the base material for powder metallurgy (PM) of ferrous components. The powder surface chemistry is characterized by a thin surface oxide layer and more thermodynamically stable oxide particulates whose extent, distribution, and composition change during the sintering cycle due to a complex set of oxidation–reduction reactions. In this study, the surface chemistry of iron and steel powder was investigated by combined surface and thermal analysis. The progressive reduction of oxides was studied using model sintering cycles in hydrogen atmospheres in a thermogravimetric (TG) setup, with experiments ended at intermediate steps (500–1300°C) of the heating stage. The surface chemistry of the samples was then investigated by means of X-ray photoelectron spectroscopy (XPS) to reveal changes that occurred during heating. The results show that reduction of the surface oxide layer occurs at relatively lower temperature for the steel powder, attributed to an influence of chromium, which is supported by a strong increase in Cr content immediately after oxide layer reduction. The reduction of the stable oxide particulates was shifted to higher temperatures, reflecting their higher thermodynamic stability. A complementary vacuum annealing treatment at 800°C was performed in a furnace directly connected to the XPS instrument allowing for sample transfer in vacuum. The results showed that Fe oxides were completely reduced, with segregation and growth of Cr and Mn oxides on the particle surfaces. This underlines the sequential reduction of oxides during sintering that reflects the thermodynamic stability and availability of oxide-forming elements.

## KEYWORDS

sintering, steel powder, surface analysis, thermal analysis, water-atomized iron powder

## 1 | INTRODUCTION

The surface chemistry of iron and steel powder used in powder metallurgy (PM) has been widely studied over the last few decades,<sup>1–3</sup> where special attention has been given to the characterization of oxide particulates that are distributed across the powder surfaces.<sup>3–5</sup>

The composition of these oxides does not necessarily correspond to the composition of the bulk metal powder, but instead reflect the ability of the elements to form thermodynamically stable oxides, and consequently, the oxides on the most common advanced PM steel grades are typically enriched in chromium and manganese.<sup>3,4,6</sup> While the nature of these oxides is in general well understood, their role in

This is an open access article under the terms of the Creative Commons Attribution License, which permits use, distribution and reproduction in any medium, provided the original work is properly cited.

© 2020 The Authors. Surface and Interface Analysis published by John Wiley & Sons Ltd

sintering is more complicated due to oxide transformation events during the heating stage of sintering, wherein oxygen from the less stable iron-rich oxides can be transferred to react with elements that form more stable oxides.<sup>5,7,8</sup> The ability to reduce oxides and subsequently remove the reaction products therefore play a crucial role in the successful sintering of PM steels.<sup>5</sup> The aim of this study is to further characterize the trajectory of oxide transformation and reduction during sintering of water-atomized iron and low-alloyed steel powder commonly used in the PM industry. For this purpose, interrupted sintering trials were conducted in a thermogravimetric analyzer (TGA) emulating a sintering furnace with well-controlled temperature and atmosphere conditions. After sintering, the samples were prepared for surface analysis by X-ray photoelectron spectroscopy (XPS). An in situ vacuum annealing of steel powder was also conducted that allowed for sample transfer in vacuum conditions prior to XPS analysis. The chemical changes revealed were then correlated to the recorded mass losses obtained by TGA to detail the progression of oxide reduction.

## 2 | MATERIALS AND EXPERIMENTAL METHODS

Two powder grades were supplied by Höganäs AB, Sweden: (i) water-atomized iron powder (nominally pure Fe) and (ii) water-atomized steel powder pre-alloyed with chromium (Fe-1.8 wt.% Cr). Due to the large specific surface area of the powder, oxygen levels in the range 0.11–0.14 wt.% (measured by LECO analysis at Höganäs AB) are typically present along with low levels of trace elements such as manganese and silicon. The sintering trials were done in a Netzsch STA F1 Jupiter<sup>®</sup> thermogravimetric analyzer. Approximately 2 g of powder per sample was put in an Al<sub>2</sub>O<sub>3</sub> crucible before loading it into the instrument. The sintering program consisted of a heating stage at 10°C/min up to a given set temperature in the range 500–1300°C, immediately followed by cooling down to room temperature at 30°C/min. The sintering atmosphere was pure hydrogen (6.0, 99.9999%) to ensure consistently strong reducing conditions. The surface chemistry was subsequently analyzed by XPS using a PHI VersaProbe III instrument with an Al K $\alpha$  source operated at 50 W. Depth profiling was avoided in this study to mitigate issues with inadvertently reducing oxides.<sup>9</sup> As-received powder and powder that was not sufficiently sintered together for handling were pressed into Al plates, while the sintered samples were fractured prior to analysis. It should be noted that the surface analyses were done on samples exposed to air when transferred between the thermogravimetric analyzer and the XPS, thus causing re-oxidation of the powder surfaces. Nevertheless, the relative intensity of the signals from the Fe 2p, Mn 2p, and Cr 2p regions will reflect the prevalence of the elements at the surface after heating to different stages. To complement the surface analysis of TG-sintered samples, steel powder was pressed onto a Cu-plate and loaded into a furnace system accessible through the XPS. A vacuum annealing experiment (800°C, 10<sup>−5</sup> Pa, 1 hr) was then performed after which the sample

was transferred back to the main chamber of the XPS for analysis without contact with air.

## 3 | RESULTS AND DISCUSSION

Figure 1 shows XPS survey scans for the iron and steel powder grades in their as-received conditions. The main difference between the grades is the significant manganese peak found for the iron powder, which is a commonly observed trace element in this type of powder grade, often in conjunction with sulphur.<sup>3</sup> No other large differences can be observed at this point.

The powder grades were then heated using model sintering cycles described previously. The results can be seen in Figure 2 showing typical thermogravimetric curves of the iron and steel powder along with the sampling points in the range 500–1300°C, which indicate where samples were collected. The first mass losses at 300–400°C are commonly attributed to the reduction of the iron-rich surface oxide layer covering most of the powder particle surfaces.<sup>10</sup> Note that this reduction event occurs about 75°C lower for the steel powder, something that is believed to be caused by the change in composition of the oxide layer. A comparable result has been shown in another study where reduction of iron oxide in hydrogen was found to be promoted by doping with chromium.<sup>11</sup> This could help explain the observed lower reduction temperature of the steel powder. The magnitude of mass loss related to the reduction below 400°C for the steel powder is also slightly smaller, indicating either a slight difference in particle size distribution or oxide layer thickness,<sup>10</sup> although the oxide layer thicknesses on both water-atomized iron and steel powder are typically considered to be similar.<sup>5,10</sup> The progressive mass loss up to the sintering temperatures in the range 700–1300°C is likely related to a combination of reduction of internal oxides and stable particulate oxides distributed on the powder particle surfaces. The clear differences in reduction behavior between the two grades

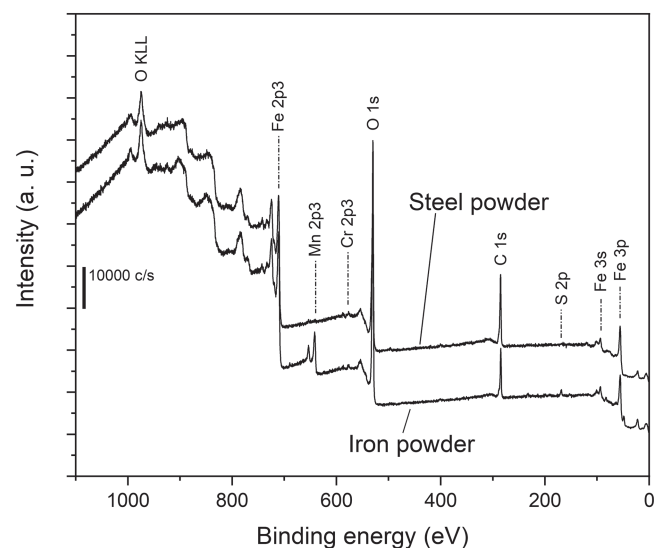
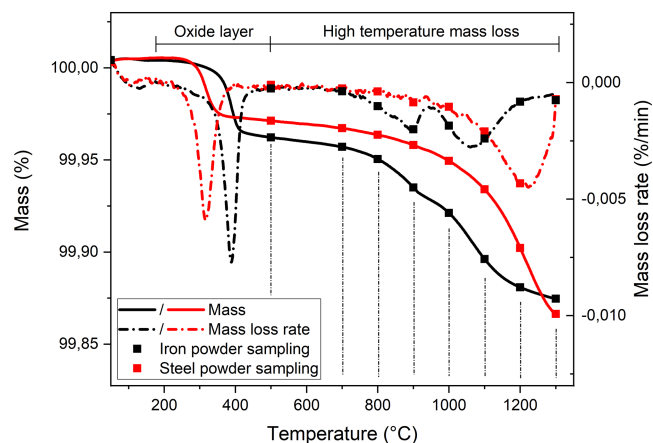


FIGURE 1 XPS survey scan of iron and steel powder



**FIGURE 2** Thermogravimetric analysis of iron and steel powder

can be explained by the difference in composition; the steel powder has a higher chromium content, which in turn translates to a larger amount of stable chromium-containing oxides that require higher temperatures for reduction. Consequently, the main reduction peaks at high temperature are situated over 100°C apart: around 1050°C and around 1200°C for the iron and steel powder, respectively. One limitation with the thermogravimetric analysis is that chemical changes with no net loss or gain in mass are not recorded, and therefore, the method cannot be used to directly study the important oxygen transfer events. For this reason, TGA was combined with XPS

to provide a more complete representation of the surface chemical changes. It should be noted that in a real industrial PM setting, the powder is compacted, which imposes additional challenges related to the decrease in porosity, which makes the removal of reduction products more difficult. This added complexity is not investigated in this study, but some details can be found elsewhere.<sup>8</sup>

Figure 3A–F shows XPS narrow scans of the iron and steel powder in their as-received conditions and after heating to 500–1300°C, that is, from a point immediately following reduction of the surface oxide layer (cf. Figure 1). The changes observed in the Fe 2p region (Figure 3A,D), with a clear shoulder on the right side of the oxide peak due to contribution from metallic Fe, are related to this reduction event. The relatively thick oxide layer on the as-received powder (5–7 nm) is being replaced by a thinner native oxide after reduction and subsequent cooling in the thermogravimetric setup. This native oxide is expected to be approximately 3 nm thick<sup>12</sup> and allows for Fe 2p photoelectrons to be detected from the metal matrix. The initial large Mn content in the iron powder (3b) is lowered slightly after heating to 500°C, one possible reason being the removal of Mn bound to  $\text{SO}_4^{2-}$  on the powder surface.<sup>3</sup> For the steel powder, a large increase in Cr in oxide state can be seen after heating to 500°C (Figure 3F). The conditions are still oxidizing for chromium at this point, but no significant diffusion should be possible to increase the content at the surface. Consequently, it is likely that chromium is present within the oxide layer or at the metal/oxide interface of the as-received powder, as has been indicated in earlier studies of Fe–Cr

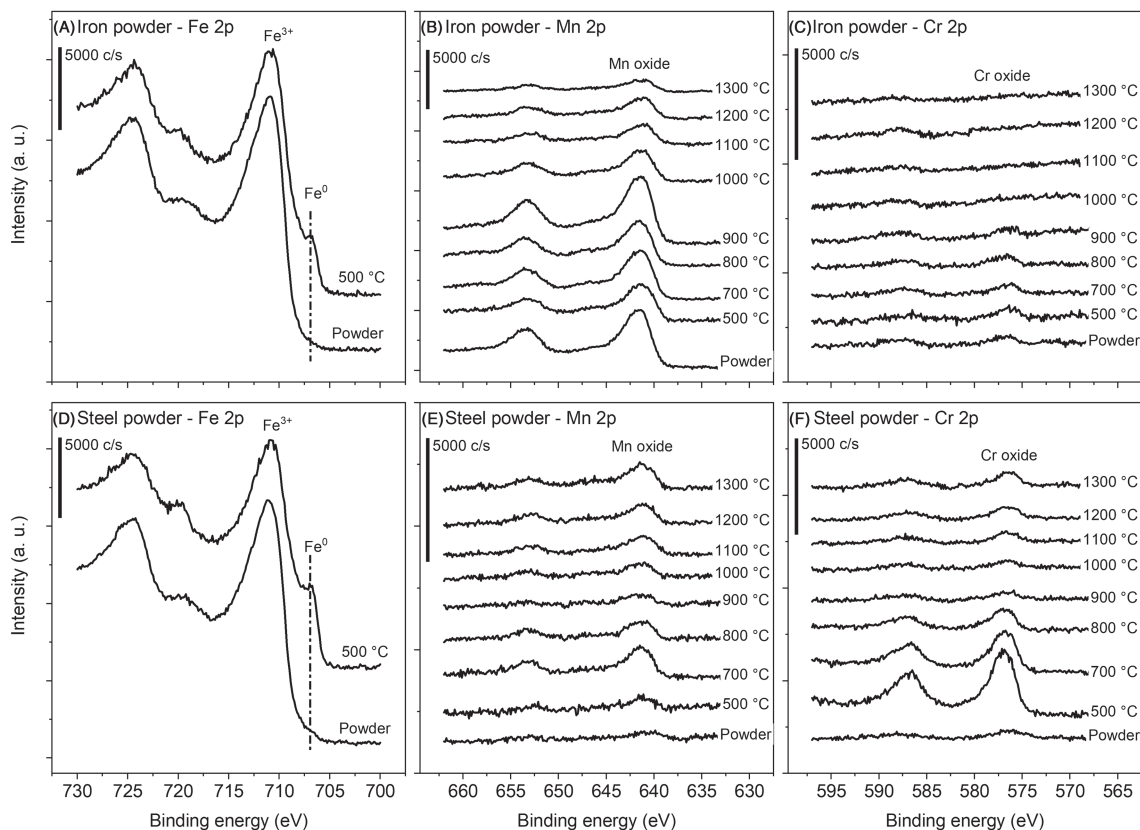


**FIGURE 3** XPS narrow scans of iron (A–C) and steel powder (D–F) of the Fe 2p, Mn 2p, and Cr 2p regions, respectively

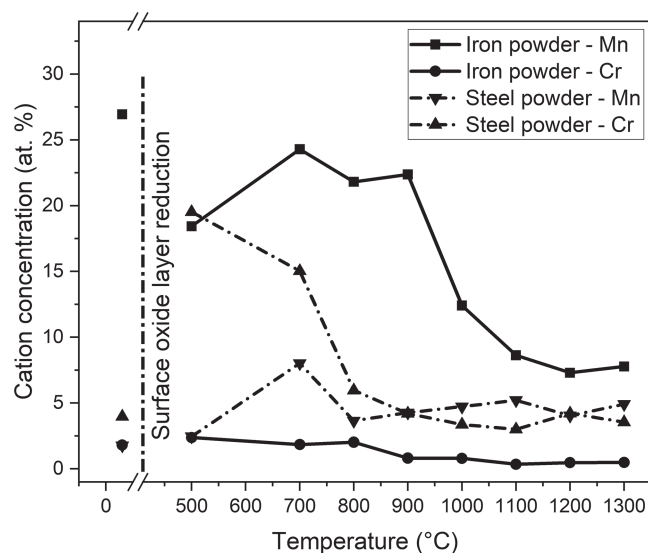


**FIGURE 4** Cation concentration versus temperature for iron and steel powder

alloys,<sup>13,14</sup> although it is believed that the current oxide layer may be too thin to observe this. Furthermore, when the easily reduced surface oxide layer is removed at lower temperatures, the thermodynamically more stable Cr oxides will remain on the surface. With further heating, the presence of Cr is then lowered due to progressive reduction of the chromium oxide. Since the iron powder only contains

trace amounts of chromium, no such surface accumulation of Cr oxide is observed after reduction of the oxide layer (Figure 3C). An increase in Mn oxide on the steel powder can be observed between 500°C and 700°C (Figure 3E), which is when a substantial lowering of the Cr oxide takes place. This change is attributed to the greater thermodynamic stability of manganese oxide causing an oxygen transfer to occur. With continued heating, the Mn oxide signal is then lowered due to reduction and then levels out. The relative intensities of the cations Fe, Mn, and Cr are plotted versus temperature in Figure 4 (Fe is balance) showing reasonably good correlation with the thermogravimetric results (Figure 1) as primarily Mn is reduced in the iron powder while both Mn and Cr are present in the steel powder.

Due to the limitations in transferring sintered samples from the thermogravimetric setup to the XPS, a vacuum annealing experiment was conducted at 800°C in a furnace that allowed for sample transfer for XPS analysis without exposure to air. The results can be seen in Figure 5. The survey scan (Figure 5A) reveals dramatic changes in the powder chemistry after annealing. From mostly showing oxide signal in the Fe 2p region, the iron oxides dissociate in the vacuum that results in mostly metallic state iron after annealing (Figure 5B). In addition, large contributions from segregated Mn and Cr in oxide state (Figure 5C,D) can now be observed along with some metallic Cr as shown by a shoulder on the low binding energy side of the Cr oxide peak (Figure 5D). The strong reducing conditions at the surface further facilitate outwards diffusion of S and Si to form sulfide and oxide, respectively, where the contribution from Si oxide also shifts

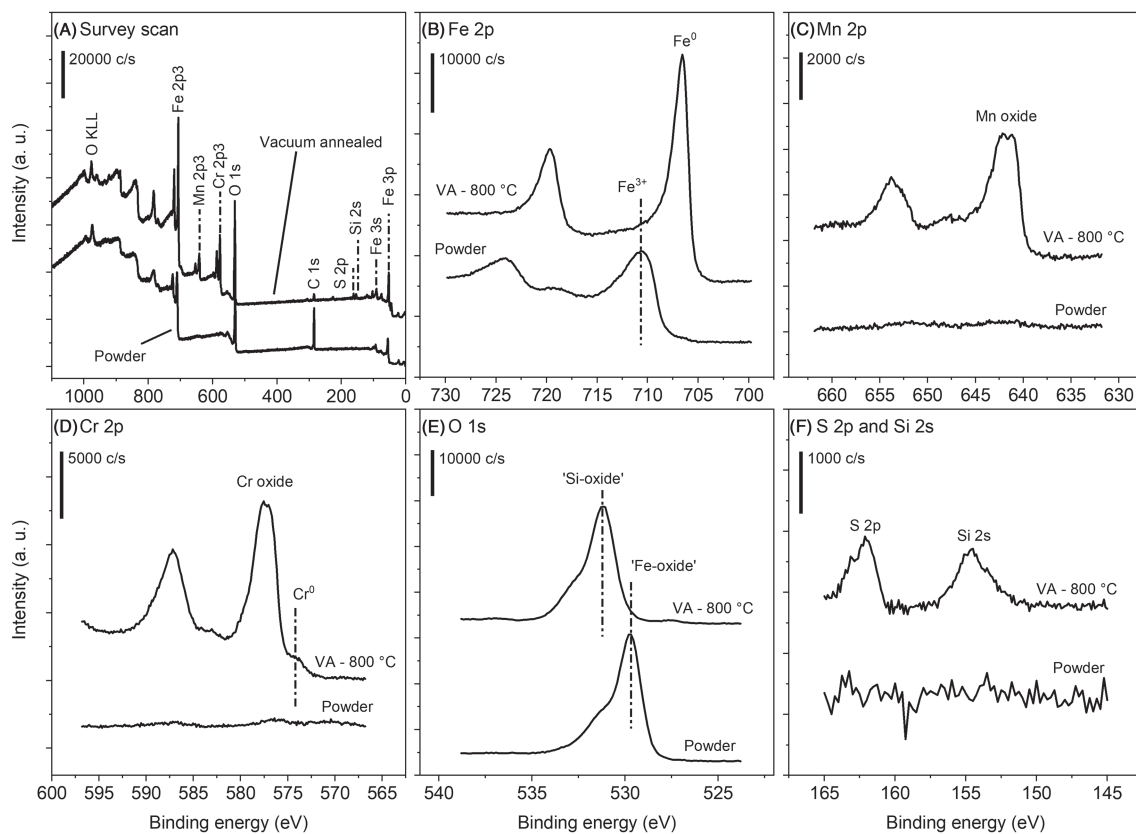


**FIGURE 5** XPS comparison of steel powder before and after vacuum annealing (VA) at 800°C

the O 1s signal to higher binding energy positions. Although the analysis of vacuum annealed powder highlights the chemical changes of a surface that was never exposed to air, sintering in hydrogen more closely represents conditions that are realized industrially. However, while the reduction processes in vacuum and hydrogen are different, the continuous reduction of oxides is expected to be similar and reflects the oxide stability and the efficiency of the reducing medium.

## 4 | CONCLUSIONS

The progressive change of surface chemistry during sintering was analyzed for water-atomized iron powder and steel powder pre-alloyed with chromium. Both grades are characterized by a thin oxide layer covering most of the powder surface with minor particulate oxides containing Mn and Cr distributed on the surface. Thermogravimetric results show a continuous decrease in sample mass during sintering, corresponding to the reduction of internal and surface oxides by hydrogen. The surface oxide layer is reduced at approximately 320°C and 395°C for the steel and iron powder, respectively. It is suggested that the difference in lower reduction temperature for the Cr-containing powder is a result of a change in the oxide layer composition. This is also indicated by the strong gain in surface content of Cr oxide immediately after oxide layer reduction for the steel powder, with no analogy for the iron powder. A progressive decrease in manganese and chromium oxides is observed with an increase in temperature, which signifies the reduction of stable oxide particulates on the surface. The vacuum annealing of the steel powder at 800°C reveals large changes in the surface chemistry of the powder and reflects the reducing conditions that dissociate iron oxides but drive a segregation of Cr and Mn to the surface of the powder particles. It is shown that the complementary use of thermogravimetric and surface chemical analysis can provide the means to assess surface chemical changes of powder during sintering under well-defined conditions.

## ACKNOWLEDGEMENTS

The authors thank the Swedish Foundation for Strategic Research (SSF) for funding and Höganäs AB for scientific cooperation. Support from Production Area of Advance, Chalmers University of Technology, is appreciated. Dr. Eric Tam is acknowledged for assistance with the vacuum annealing experiments.

## ORCID

Johan Wendel  <https://orcid.org/0000-0003-3659-0498>

Swathi K. Manchili  <https://orcid.org/0000-0002-7170-6030>

Yu Cao  <https://orcid.org/0000-0002-1965-5854>

Eduard Hryha  <https://orcid.org/0000-0002-4579-1710>

Lars Nyborg  <https://orcid.org/0000-0002-1726-5529>

## REFERENCES

1. Danninger H, Gierl C, Kremel S, Leitner G, Yu Y. Degassing and deoxidation processes during sintering of unalloyed and alloyed PM steels. *Powder Metall Prog.* 2002;2:125-140.
2. Danninger H, Gierl C. New alloying systems for ferrous powder metallurgy precision parts. *Sci Sinter.* 2008;40(1):33-46.
3. Hryha E, Gierl C, Nyborg L, Danninger H, Dudrova E. Surface composition of the steel powders pre-alloyed with manganese. *Appl Surf Sci.* 2010;256(12):3946-3961.
4. Chasoglou D, Hryha E, Norell M, Nyborg L. Characterization of surface oxides on water-atomized steel powder by XPS/AES depth profiling and nano-scale lateral surface analysis. *Appl Surf Sci [Internet]. Elsevier B.V.;* 2013;268:496-506. Available from: <https://doi.org/10.1016/j.apsusc.2012.12.155>
5. Hryha E, Nyborg L. Oxide transformation in Cr-Mn-prealloyed sintered steels: thermodynamic and kinetic aspects. *Metall Mater Trans a Phys Metall Mater Sci.* 2014;45(4):1736-1747.
6. Danninger H, Gierl-mayer C. Advanced powder metallurgy steel alloys. *Adv. Powder Metall. Prop. Process. Appl.* 2013;149-201.
7. Chasoglou D, Hryha E, Nyborg L. Effect of sintering atmosphere on the transformation of surface oxides during the sintering of chromium alloyed steel. *Powder Metallurgy Progress.* 2009;9:141-155.
8. Vattur Sundaram M, Hryha E, Nyborg L. XPS analysis of oxide transformation during sintering of chromium alloyed PM steels. *Powder Metall Prog [Internet].* 2014;14:85-92. Available from: [http://www.imr.saske.sk/pmp/issue/2-2014/PMP\\_Vol14\\_No2\\_p\\_085-092.pdf](http://www.imr.saske.sk/pmp/issue/2-2014/PMP_Vol14_No2_p_085-092.pdf)
9. Yamashita T, Hayes P. Analysis of XPS spectra of Fe<sup>2+</sup> and Fe<sup>3+</sup> ions in oxide materials. *Appl Surf Sci.* 2008;254(8):2441-2449.
10. Wendel J, Shvab R, Cao Y, Hryha E, Nyborg L. Surface analysis of fine water-atomized iron powder and sintered material. *Surf Interface Anal.* 2018;50(11):1065-1071.
11. Saharuddin TST, Samsuri A, Salleh F, et al. Studies on reduction of chromium doped iron oxide catalyst using hydrogen and various concentration of carbon monoxide. *Int J Hydrogen Energy [Internet]. Elsevier Ltd.* 2017;42(14):9077-9086. Available from: <https://doi.org/10.1016/j.ijhydene.2016.08.151>
12. Suzuki S, Ishikawa Y, Isshiki M, Waseda Y. Native oxide layers formed on the surface of ultra high-purity iron and copper investigated by angle resolved XPS. *Mater Trans JIM.* 1997;38(11):1004-1009.
13. Olefjord I. ESCA-studies of the composition profile of low temperature oxide formed on chromium steels—I. Oxidation in dry oxygen. *Corros Sci.* 1975;15(6-12):687-696.
14. Tjong SC, Eldridge J, Hoffman RW. AES studies of the oxides formed on iron-chromium alloys at 400°C. *Appl Surf Sci.* 1983;14(3-4): 297-306.

**How to cite this article:** Wendel J, Manchili SK, Cao Y, Hryha E, Nyborg L. Evolution of surface chemistry during sintering of water-atomized iron and low-alloyed steel powder. *Surf Interface Anal.* 2020;52:1061-1065. <https://doi.org/10.1002/sia.6852>